Journal of Materials Chemistry A

Accepted Manuscript

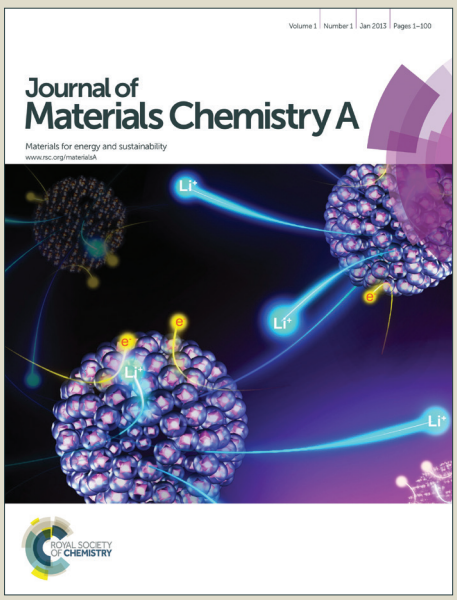

ROYAL SOCIETY OF CHEMISTRY

www.rsc.org/materialsA

Polydopamine particles for next-generation multifunctional biocomposites

Shuqiang Xiong[a], Yan Wang*[b], Junrong Yu[a], Lei Chen[b], Jing Zhu[b] and Zuming Hu*[a]

a State Key Laboratory for Modification of Chemical Fibers and Polymer Materials, Donghua University, 201620, Shanghai (P. R. China)

b College of Material Science and Engineering, Donghua University, 201620, Shanghai (P. R. China)

**Corresponding authors. Tel.: +86-21-67792944. Fax: +86-21-67792945.*

E-mail: wy@dhu.edu.cn (Y. Wang); hzm@dhu.edu.cn (Z. Hu)

Abstract

To support the rapid advancements in the field of biocomposites, it is necessary to exploit novel fillers that are biocompatible, multifunctional, and easy to obtain. In this work, Polydopamine particle (PDAP) was reported as filler for constructing polymer composites. PDAPs with average diameters of about 1040 and 310 nm were first prepared by a convenient oxidative polymerization of dopamine, then PDAP/poly (vinyl alcohol) (PVA) composites were prepared through traditional solution-casting method. The measurements of the resultant composites confirmed the strong interactions between PDAPs and PVA chains, and the good dispersion state of PDAPs in the matrix. It was found that the PDAPs could promote the crystallization of PVA, and thus greatly improved the mechanical properties of composites. TGA results showed that both the initial and maximum decomposition temperatures of PVA were significantly increased by the addition of PDAPs. Moreover, the composites showed superior antioxidant property and UV-shielding efficiency as compared to neat PVA. The effect of particle size on the reinforcement effect was also evaluated. The results suggested that PDAP could be a good candidate for multifunctional composites.

1. Introduction

Polymer based composites have attracted tremendous attention in recent years because of the combination of advantages from both components. The continuous polymer phase renders processability and stability to the composites, while the reinforcement phase endows these composites with novel functionalities, such as electrical conductivity, antibacterial properties, UV-resistance, and flame-resistance, etc[1-4]. Up to now, majority of reported composites were filled with nanoscale or sub-microscale inorganic nanomaterials, such as carbon nanotube, graphene, clay and metal particles[5-8]. The incorporation of these inorganic particles into polymers has been demonstrated to significantly improve the physical properties of matrices. Therefore, the inorganic nanomaterials based polymer composites hold great promise in various applications related to their mechanical, electrical, thermal or optical properties. However, for safety consideration, these inorganic fillers are not suitable for composites in some bio-related applications, because most of the inorganic particles are not biodegradable or biocompatible, or even toxic to human[9-11]. In this context, biopolymers, such as cellulose whisker[12], chitin[13], and collagen[14] have been exploited as reinforcement in composites. However, these fillers could hardly provide improvements other than mechanical properties due to the lack of functionalities and the intrinsic poor thermal stabilities themselves[15-18].

On the other hand, dopamine is an important neurotransmitter containing amine and catechol groups that are present in a lot of aminals. Since the discovery that dopamine could self-polymerization in alkaline solution that mimic mussel-adhesive proteins[19], great efforts have been paid to employ mussel-inspired polydopamine for surface

coating[20-22]. Although the exact mechanism of self-polymerization of dopamine is unclear, and the structure of polydopamine is still under debate[23, 24], the excellent properties such as adhesive properties, biocompatibility and antioxidant properties, of polydopamine have been demonstrated, which have stimulated researchers to exploit polydopamine in various applications. For example, Ryou et al. reported the use of polydopamine coated polyethylene as separators for Li-ion battery[25]; Cui et al. have prepared polydopamine capsules for drug delivery[26]; Feng et al. used polydopamine as precursor for preparation of stretchable and transparent conductors[27].

Polydopamine is also emerged as a promise material in the field of polymer composites. For instance, polydopamine coated boron nitride nanotubes[28], carbon nanotubes[29,30], graphenes[31-33] and clays[34-36] have been investigated as reinforcement for polymers. The modification of the inert surfaces of inorganic nanoparticles could not only improve the dispersion state, but also facilitate stress-transfer between fillers and matrix. Most importantly, the polydopamine coatings on the filler surfaces could even add new functions to the polymer matrix, such as UV-shielding and radical-scavenging[35]. However, the major reinforcements and functions were still provided by the inorganic particles, the capability of polydopamine for polymer reinforcement was still unexploited.

Structurally, polydopamine is similar to melanin, which is a biopolymer that possessed intriguing physical properties[37], therefore, polydopamine should share some common properties of natural melanin. However, natural melanin is hard to be isolated without altering its physiochemical properties, the insoluble characteristic of natural melanin also hampers its use in polymer composites[38]. Recently, Shanmuganathan et al. demonstrated that synthetic melanin powders from oxidation of 3,4-dihydroxy-L-phenylalanine (L-

Dopa) significantly improved the thermal and thermooxidative stability of poly(methyl methacrylate) (PMMA), suggesting the great potential of melanin-like polymers for reinforcement of polymer composites[39]. However, these synthetic melanins could only be synthesized in some toxic solvents such as N,N-dimethylformamide (DMF) and dimethyl sulfoxide (DMSO), and most synthetic melanins were insoluble in water[40, 41]. In particular, the shapes and sizes of these synthetic melanins, which were very important to prepare composites with predictable and reproducible properties, could hardly be controlled. In contrast, recent studies showed that melanin-like polydopamine particle (PDAP) could be prepared in environmentally friendly solvents and disperse in a variety of solvents including water due to the polar functional groups on PDAP surfaces[38,42,43]. The sizes could also be readily adjusted by modulating the synthetic parameters. All these features make PDAPs very attractive fillers for constructing polymer composites, especially with bio-related applications.

Given the above mentioned consideration, here we reported the first attempt on fabricating PDAP-based polymer composites. Poly(vinyl alcohol) (PVA) was chosen as model polymer matrix because it is a water-soluble, biocompatible polymer with good physical properties, and it is been widely used as fibers, films, coatings and adhesives[44,45]. The rich hydroxyl groups of PVA could also strongly interact with PDAPs. If PDAPs could further improve the physical properties, and introduce new functions to PVA, the range of applications could be further widened. In this paper, PDAPs with two distinguishable sizes were first prepared by a method developed by Ai et al. in order to investigate the effect of particle sizes on the reinforcement efficiency[43]. PDAP/PVA composites were then prepared by simple solution-casting and tested by a variety of

methods. The results showed that PDAP was indeed an excellent candidate as filler to improve the thermal, mechanical, antioxidant and UV-shielding performance of polymers.

2. Experimental

2.1. Materials.

Dopamine hydrochloride was purchased from J&K Chemical Technology. PVA (1750±50, 99%) and ammonium hydroxide (25%-28%) were obtained from Sinopharm Chemical Reagent Co., Ltd (SCRC). Alcohol (99.7%) was obtained from Yang Yuan Chemical Reagent Co. 1,1-Diphenyl-2-picrylhydrazyl radical (DPPH) was purchased from Sigma Company, USA. All reagents were used as received without further purification.

2.2. Synthesis of PDAP with Different Sizes.

PDAPs with different sizes were prepared by oxidative polymerization of dopamine in alkaline water-ethanol solution[43]. The detailed procedure is as follows: ethanol(40 ml), deionized water (90 ml) and required amount of ammonium hydroxide (0.6 or 1.5 ml) were mixed under mild stirring. Dopamine hydrochloride solution (50mg/ml, 10ml) was then added in the above water-ethanol solution. The reaction was allowed to proceed for 30 h. PDAPs were then obtained by centrifugation and washed with water for 3 times.

2.3. Preparation of PDAP/PVA Spheres Composites.

Required amount of PDAPs were dispersed in 8ml water and sonicated for 30 min. Then, 0.9 g PVA was added to the dispersion of PDAP and stirred for 2 h at 90 ℃. After that, the homogeneous mixture was poured into polished stainless steel plate and dried at 60 ℃ until the weight become constant. The composite films were uniform with an average thickness of 80 μm.

2.4. Characterization

Fourier transform infrared (FT-IR) spectra were recorded on a perkin-Elmer Paragon 1000 FTIR spectrometer. Thermogravimetric analysis (TGA) was performed in nitrogen with a Perkin-Elmer TGA2050 instrument at a heating rate of 20 ℃/min. The glass-transition temperature (*Tg*), melting temperature (*Tm*), crystallization temperature (*Tc*) and degree of crystallinity (*Xc*) of samples were investigated by differential scanning calorimetry (DSC) using a Mettler DSC822 instrument. The heating rate was 10 ℃/min and the cooling rate was 20 ℃/min. The fracture surfaces of composite films were observed by a FEI SIRION field emission scanning electron microscope (FESEM). Transmission electron microscopy (TEM) images were obtained by JEOL2100F. UV-vis spectra of composite films were recorded by a Shimadzu 2550 UV-vis spectrometer. Tensile measurements were performed with an Instron 4465 instrument at room temperature with humidity about 50% at a crosshead speed of 40 mm/min, the initial gauge length and width were 60 and 4 mm.

Free radical scavenging activity of PDAP/PVA was evaluated by DHHP assay according to the methods reported in the literature with slight modification[46,47]. In detail, each composite samples (5 mg) were stirred in 6ml water for 24 h. Then 2 ml freshly prepared DPPH solution (0.01 mM) in DMF was added in the composite solutions. The scavenging activity was evaluated by monitoring the absorbance decrease at 516 nm after it stored in dark for 20 min. DPPH radical scavenging activity was calculated as I=[1-(Asample-Ablank)/Acontrol]×100%, where Acontrol is the absorbance of DPPH solution without samples, Asample is the absorbance of the samples mixed with DPPH solution, and Ablank is the absorbance of the samples themselves without DPPH solution.

3. Results and Discussion

3.1. Synthesis and Characterization of PDAPs.

The method developed by Ai et al. was employed to prepare PDAPs because it is very simple without the use of any toxic reagent, and the particle sizes could be readily controlled by changing the amount of ammonium hydroxide, which was very important for controllable fabrication of composites. During the preparation process, dopamine was spontaneously oxidized and polymerized into spherical PDAPs via intra/intermolecular cross-linking[38]. The particle sizes could be modulated by controlling the polymerization rate in solutions with different pH[43]. In this work, PDAPs with two different sizes were prepared. Hereafter, PDAP with bigger size was denoted as PDAP1, the smaller one was denoted as PDAP-2.

SEM images (Figure 1a and 1b) demonstrated the successful synthesis of PDAPs. Both the PDAP-1 and PDAP-2 were uniformly spherical particles. TEM images (Figure 1c and 1d) also support the uniform sizes of PDAP-1 and PDAP-2, and the sizes are identical to the observation of SEM characterization. However, the high magnified TEM images (Figure 1e and 1f) show that PDAP-1 has relatively smooth surface, while the surface of PDAP-2 is a little rougher with some lumps across the surface, which were attributed to the fast polymerization rate of dopamine in solution with high pH. The sizes were then calculated based on the SEM and TEM observations. The statistics of diameter calculated from a large number (~150) of particles of PDAP-1 and PDAP-2 are presented in Figure 1g and 1h, respectively. It can be seen that the diameters displayed a Gaussian

distribution with average values of about 1040 and 310 nm for PDAP-1 and PDAP-2, suggesting the monodisperse nature of PDAPs[42].

Because the surface characteristics and thermal property of fillers could significantly influence the performance of composites, we therefore carried out FT-IR and TGA analysis on PDAPs. Figure 2a presents the FT-IR spectra of PDAP-1 and PDAP-2. Both PDAP-1 and PDAP-2 have broad bands in the range between 940 and 1800 cm^{-1} with no distinguishable peaks due to the highly complex structure of polydopamine, which was consistent with previous studies[38,48]. The peaks centered at around 3413 cm^{-1} were ascribed to nitrogen–hydrogen/oxygen–hydrogen bonds. Moreover, the similar spectra of PDAP-1 and PDAP-2 suggest the similar surface properties of them. TGA analysis (Figure 2b) shows that no well-defined decomposition temperature can be found in PDAPs, in contrast to dopamine. The multistep degradation behavior of PDAPs is similar to that of natural and synthetic melanin[39], suggesting again the heterogeneous structure of polydopamine and the presence of different chemical groups. The residuals of PDAP-1 and PDAP-2 at 650 ℃ were 64.7% and 61.1%, respectively, both were much higher than that of dopamine (22.7%), suggesting the carbonization of PDAPs[43].

3.2.Preparation of PDAP/PVA Composites.

Because of the attached hydrophilic surface groups, PDAPs have good dispersibility in water. Therefore, PDAP/PVA composites could be easily prepared by solution-casting method. The morphologies of composite films were first characterized by SEM. The fracture surface of PVA and composites are shown in Figure 3. In contrast to the smooth surface of neat PVA (Figure 3a), there are many circular protrusions across the surface of composites, which were undoubtedly the PDAPs. For composites with filler loadings of 5

wt%, both PDAP-1 and PDAP-2 were uniformly distributed in the composites. However, when the loading of PDAPs increased to 10 wt%, some small aggregations were found in PDAP-2/PVA, as indicated by the arrows. As the content of PDAPs increased to 15 wt%, aggregations in PDAP-2/PVA were more serious, while PDAP-1 was still homogenously dispersed in composite. The larger surface area and surface tension of smaller particles were thought to be the reason for the aggregation of PDAP-2 in composite with high filler loading[49].

Besides the dispersion state, the interaction between fillers and matrix was another important factor that influenced the properties of composites. Because there were many hydrophilic groups attached on the surface of PDAPs, it is reasonable that PDAPs could strongly bind to the hydroxyl groups of PVA. FT-IR measurement was conducted to demonstrate this point, as shown in Figure 4. The –OH stretching in the spectra of PDAP-1/PVA and PDAP-2/PVA composites with 10wt% fillers are located at 3276 and 3274 cm^{-1}, shifting to lower wavenumber as compared to that of neat PVA (3303 cm^{-1}). The –C-OH stretching also shifts from 1096 cm^{-1} of PVA to 1086 cm^{-1} in composites. Both of these phenomena demonstrate the existence of hydrogen-bonding between the hydroxyl groups of PVA and the functional groups of PDAPs[50,51].

3.3. Thermal Properties of PDAP/PVA Composites.

As is known, the incorporation of fillers into matrix could affect the chain mobility of polymers, thus influence the thermal behaviors, especially for semicrystalline polymers, therefore, we have conducted DSC measurements on PDAP/PVA composites, both heating and cooling scans were recorded, the values are listed in Table 1. Figure 5a and 5b presents the low-temperature portion of heating scan, from which we can compare the

Tg of PVA and their composites. PVA shows a *Tg* of 43.3 °C, suggesting the plasticization effect of humidity[52]. it is found that the *Tg* increases with the increase of filler loadings. When the content of PDAPs increased to 15 wt%, the PDAP-1/PVA and PDAP-2/PVA composites show maximum *Tg* of 47.4 and 48.6 °C. From the configurational entropy theory of the glass transition, the increased *Tg* is a result of the restricted motion of polymer chains[53,54]. Therefore, the Tg results suggested again the strong interactions between PDAPs and PVA chains.

Besides the *Tg*, the *Tm* of PVA was also increased upon addition of PDAPs, as shown in Figure 5c and 5d. The *Tm* for the PDAP-1/PVA and PDAP-2/PVA loaded with 15 wt% fillers were determined to be 236.2 and 234.6 °C, while it is 231.3 °C for neat PVA. Moreover, a considerable increase in crystallinity of PVA was also observed. Compared to neat PVA (ΔHm=34.7 J/g), the crystallinity of PDAP-1/PVA and PDAP-2/PVA composites with 15 wt% fillers increased from 25.0% to 45.4% and 42.3% (considering the the enthalpy of fusion of PVA is 138.6 J/g), respectively, suggesting that PDAPs promoted crystallization of PVA. Similar nucleation effect has also been reported for proteins such as collagen[55]. Since polydopamine is structurally similar to mussel adhesive protein, it is not surprise that PDAPs could promote the crystallization of PVA. The improved crystallinity can also be reflected by the increase of melt temperatures.

The nucleation effect of PDAPs on PVA was even more pronounced during the cooling process, as shown in Figure 5e and 5f. The *Tc* of PVA was about 165.9 °C, and the exothermic enthalpy ($\Delta Hm2$) was 20.7 J/g, corresponding to crystallinity of 14.9%. After the incorporation of PDAPs, the *Tc* increased significantly. For example, the *Tc* for composites with 15 wt% PDAP-1 and PDAP-2 were 189.8 and 190.3 °C, the $\Delta Hm2$ were

also increased to 51.0 and 45.5 J/g, corresponding to crystallinity of 36.8% and 32.8%, respectively, suggesting again the PDAPs might act as nuclei and increase the crystallization growth rate. Moreover, as the content of PDAPs increases, the crystallization peaks of composites become narrow, indicating the strong noncovalent binding between PDAPs and polymer main chains result in higher molecular conformational ordering, crystals in composite were more regular than those in neat PVA[56].

However, although the PDAP-1 and PDAP-2 have the same effect on the thermal behavior of PVA, there is no distinguishable difference between PDAP-1/PVA and PDAP-2/PVA composites with the same loading of fillers. For polymer composites, it is suggested that smaller fillers should have larger surface areas, and thus should restricted more polymer chains. In this work, as PDAP-1 and PDAP-2 have similar surface functionalities, thus it is expected the size of PDAP might be the dominant factor that control the reinforcement effect, but the DSC results show no big difference between PDAP-1 and PDAP-2 as reinforcement agent. We thought the following reasons might be account for this phenomena: 1) the sizes of PDAP-1 and PDAP-2 were both in the sub-micrometer range, thus the differences in PDAP-1/PVA and PDAP-2/PVA were not big enough to detect by DSC; 2) smaller fillers are easier to aggregate because of their larger surface tension as revealed by SEM images in Figure 3.

TGA was then employed to evaluate the thermal stabilities of PVA and PDAP/PVA composites, the TGA and differential thermal gravity (DTG) curves are shown in Figure 6, the onset decomposition temperatures (*Ts*) and maximum decomposition temperatures (T_{max}) are listed in Table 2. For neat PVA, the *Ts* is about 248.3 °C, while the T_{max} of

PVA appears at about 263.3 °C, corresponding to the elimination of side hydroxyl groups and partial chain-scission. A small peak at about 450 °C can also been found in the DTG curve, which can be attributed to the pyrolysis of the polymer backbone[57,58]. With the addition of PDAP-1 and PDAP-2, the *Ts* gradually shift toward high temperature and arrived the maximum values of 277.5 and 278.1 °C for composites with 15 wt% filler, respectively. The T_{max} were also significantly increased to 309.3 and 305.9 °C for PDAP-1/PVA and PDAP-2/PVA composites with 15 wt% fillers. However, the second decomposition temperature was nearly unchanged at about 450 °C.

The improvement of thermal stability of polymer by incorporation of fillers has been frequently reported. The mechanisms behind the improvement were always described as the inhibited motion of polymer chains caused by the interactions between polymer chains and fillers, the delayed decomposition rate caused by tortuous pathway for the volatile degradation products, and the trapping of free radicals generated by chain-scission[59-61]. Considering the degradation pathway of PVA, the major decomposition at 263.3 °C was the elimination of hydroxyl groups and the chain-scission. Therefore, it is reasonable that the strong interactions between PVA and hydrophilic PDAPs could retard the decomposition of hydroxyl groups. Moreover, a recent study carried out by Shanmuganathan et al. suggested that melanin-like particles could scavenge radicals by radical addition or electron-transfer process, thus it is also possible that PDAPs could eliminate the free radicals generated by the breaking of C–C bonds, and block the chain-scission depolymerization[39]. However, at higher temperature, because of the vigorous pyrolysis of PVA backbone, the PDAPs have no effect on decomposition at this stage.

Moreover, in contrast to the DSC measurements, which could not distinguish the difference between PDAP-1/PVA and PDAP-2/PVA composites, it is found that the T_{max} of PDAP-1/PVA was slightly lower than that of PDAP-2/PVA when the content of filler was lower than 10wt%, this might be due to the higher surface area of small particles, which could react with more radicals. However, at 15wt% loading, the aggregation of PDAP-2 was more serious than PDAP-1 because the small size, thus the performance of PDAP-1/PVA was better than PDAP-2/PVA.

3.4. Radical-Scavenging Activity of PDAP/PVA Composites.

The antioxidant properties of polymer films are very important for applications such as food packaging to prevent foods from oxidation[62]. To improve the antioxidant properties of polymers, researchers have incorporated many type of antioxidants, typically phenolic compounds[63,64], into polymer matrix. The phenolic compounds could easily quench the active radicals via electron transfer process. As PDAP contains many phenolic groups, it is natural that PDAP should be good antioxidant as additive for packaging materials. In fact, the radical-scavenging ability of PDAP has already been demonstrated[35,38]. Here we would like to see if the PDAPs could maintain their antioxidant property in composites.

The stable DPPH radicals were used to evaluate the radical scavenging ability of composites. The scavenging activities of PVA and composites are compared in Figure 7. The results showed that the scavenging activities of films dramatically increased with increasing content of PDAPs. PVA without PDAPs showed scavenging activity of only about 3.5%, while the activities increased to 88.4% and 89.0% for PDAP-1/PVA with 15 wt% fillers and PDAP-2/PVA with 10 wt% fillers, suggesting the great potential of

PDAPs as antioxidant additives for polymer composites in the field of food packaging. Moreover, the PDAP-2 showed better activity than PDAP-1 in composites with loadings lower than 10 wt%, suggesting the larger surface area of PDAP-2 was of benefit to improve the antioxidative properties. However, in composites with 15 wt% fillers, the improvement in scavenging activity of PDAP-2/PVA was comparable to that of PDAP-1/PVA, indicating the activity of PDAP-2 has been compromised by the aggregations.

3.5. UV-shielding of PDAP/PVA Composites.

A major function of melanin in skin is to protect animals from UV irradiation. Therefore, it can be expected that the incorporation of PDAPs into polymers could enhance the UV-shielding efficiency of composites, which was crucial for protective coating and packaging applications[65]. The UV-Vis transmittance spectra of composite films (~30 μm) are shown in Figure 8. PVA shows good transparence in the visible light range, but can only block UV light up to 340nm with a transmittance of 85% at 400 nm. By incorporating PDAPs into the matrix, the colorless PVA gradually changed to pale yellow with low content of PDAPs, then transferred to brown as the contents of PDAPs further increased. It was found that UV light was effectively absorbed by the composites. For example, the transmittance of PDAP-1/PVA composites with 5 wt% fillers is only 28%, and further decrease to 18% and 2% for composites with 10 wt% and 15 wt% fillers, respectively. Moreover, it is found that the UV-shielding efficiency of PDAP-2 was even more profound than that of PDAP-1. With only introduction of 1 wt% PDAP-2, the transmittance at 400 nm decreased to 40% with slightly deterioration of transparence at visible light range, and it significantly decreased to 5% with the addition of 5 wt%

PDAP-2 with a modest transparence at visible light range. The UV light was nearly completely blocked in composite with 10 wt% PDAP-2.

It is known that the UV screening mechanism of organic agent is the absorption of UV light and the energy transformation by chromophores such as phenol, quinone, -C=N and -C=O groups[66]. The smaller particles have larger surface areas and thus more functional groups attached on the surface. Moreover, the larger interface areas in PDAP-2/PVA could also scatter or reflect more UV light. However, for PDAP-1/PVA composites, the light reflection was thought to be the main reason for the decreased UV transparence, because the sizes of PDAP-1 is large than the wavelength of UV and visible light. Therefore, PDAP-2 shows better performance in UV-shielding composites. It is also noted that as compared to some inorganic nanoparticles (TiO_2 or ZnO), it required more PDAPs in composites to achieve the same effect of UV-shielding, and the transparence in visible light range was not as good as inorganic particle filled composites[67,68]. However, the inherent photocatalytic activity of the metal oxide would result in the decomposition of polymer matrix[69], by using our PDAPs could avoid the risks. In addition, the low-cost, biocompatibility, and environmentally friendly synthetic procedure were the main advantages of PDAPs for use in human health protection areas.

3.6. Mechanical Properties of PDAP/PVA Composites.

The nucleation effect of PDAPs on PVA was also expected to bring positive impact on the mechanical properties. Therefore, we have carried out tensile testing on the composites. For accuracy, at least four strips were tested for each sample. The average modulus and tensile strength are compared in Figure 9, and the values are listed in Table 2. The modulus and strength of PVA are 1.12 GPa and 37 MPa, which were comparable

to previous researches[70,71]. As expected, the addition of PDAPs indeed improved the mechanical properties of PVA. For example, the modulus and strength of PDAP-1/PVA with 15 wt% fillers are 1.77 GPa and 61 MPa, corresponding to improvements of 58.0% and 64.9%, respectively. Also, the PDAP-2/PVA with 15 wt% fillers are 1.72 GPa and 59 MPa, corresponding to improvements of 53.6% and 59.0%, respectively. However, the ultimate strains of composites are lowered with the addition of PDAPs.

The results clearly demonstrated the improved mechanical properties of PVA by the addition of PDAPs. However, it is hard to conclude that PDAPs are good mechanical reinforcement agents for other polymers currently, because the crystallinity of PDAP/PVA composite was much higher than that of pure PVA. Since the crystals were intrinsically much stronger than amorphous counterpart, it is reasonable that the composites with higher degree of crystallinity were stronger and stiffer than PVA with lower degree of crystallinity[72]. In spite of increased crystallity, the PDAP should also contribute to the enhanced mechanical properties. In fact, Yang et al. have recently reported that the modulus of polydopamine thin film was about 10 GPa[73]. We thought the modulus of PDAPs was similar to this value because of their similar chemical structures. Although this value is not much higher than the modulus of many commercial polymers, large amount of fillers could also significantly improve the mechanical properties based on a simple mixing rule for the composite. For example, also the difference in crystallities between PDAP-2-10wt% and PDAP-2-15wt% was only 0.5%, the modulus and strength of PDAP-2-15wt% are both much higher than PDAP-2-10wt%. Therefore, the improvement of mechanical properties of PVA in this work is mainly attributed to the combination of increased crystallinity induced by PDAPs and the mechanical

reinforcement effect of PDAP. Nevertheless, the actual effect of PDAPs on the mechanical reinforcement of polymers was expected to be unraveled in future work by using amorphous polymer matrix.

4. Conclusions

In conclusion, PDAPs were used as fillers for polymer composites for the first time. By a convenient solution-casting method, PDAP/PVA composite films with different filler sizes and contents were fabricated. The crystallinity of PVA was increased due to the nucleation effect of PDAPs. As a result of the promoted crystallinity, the mechanical properties of composites were greatly improved. The PDAPs could also significantly increase the decomposition temperature of PVA by more than 40°C with the addition of 15wt% fillers due to the strong interaction between PDAPs and polymer chains, and the radical trapping effect of PDAPs. Moreover, PDAPs provided antioxidant property and UV-resistance to PVA simultaneously. In addition, it was demonstrated that PDAPs with smaller size showed better performance than bigger ones in improving the thermal stability, antioxidant properties and UV-shielding efficiency of PVA when the fillers were homogeneously dispersed in the matrix due to their larger surface area, which could react with more sensitive radicals and absorb more UV light. However, it was noted that the small particles would aggregate in matrix with high loadings, which might compromise the positive effect of fillers. Therefore, to fully exploit the potential of PDAP on reinforcement of polymers, it is necessary to develop other delicate strategy, such as surface modification of PDAP with polymers, to fabricate homogenous composites with high filler contents. Nevertheless, the good reinforcement effect as demonstrated in this work, combined with their facile synthesis, good dispersibility,

controllable sizes, and biocompatibility, make PDAP a good candidate for constructing multifunctional composites for many applications, especially in bio-related fields.

Acknowledgements

The authors thank the National 973 Project of China (no. 2011CB606103), the National 863 Project of China (no. 2012AA03A212), the National Nature Science Foundation of China (no. 51203019), and the Fundamental Research Funds for the Central Universities (no. 11D10625) for the support.

References

1. Z. Spitalsky, D. Tasis, K. Papagelis and C. Galiotis, *Prog. Polym. Sci.*, **2010**, *35*, 357–401.
2. M. S. A. S. Shah, M. Nag, T. Kalagara, S. Singh and S. V. Manorama, *Chem. Mater.*, **2008**, *20*, 2455–2460.
3. M. E. Calvo, J. R. C. Smirnov and H. M ǵuez, *J. Polym. Sci., Part B: Polym. Phys.*, **2012**, *50*, 945–956.
4. G. Laufer, C. Kirkland, A. A. Cain and J. C. Grunlan, *ACS Appl. Mater. Interfaces*, **2012**, *4*, 1643 – 1649.
5. M. F. Variava, T. L. Church, A. T. Harris and A. I. Minett, *J. Mater. Chem. A*, **2013**, *1*, 8509-8520.
6. H. Kim, A. A. Abdala and W. C. Macosko, *Macromolecules*, **2010**, *43*, 6515–6530.
7. N. Bitinis, M. Hernandez, R. Verdejo, J. M. Kenny and M. A. Lopez-Manchado, *Adv. Mater.*, **2011**, *23*, 5229–5236.
8. G. V. Ramesh, S. Porel and T. P. Radhakrishnan, *Chem. Soc. Rev.*, **2009**, *38*, 2646–2656.
9. Y. Liu, ; Y. L. Zhao, B. Y. Sun and C. Y. Chen, *Acc. Chem. Res.*, **2013**, *46*, 702–713.
10. O. Akhavan and E. Ghaderi, *ACS Nano*, **2010**, *4*, 5731–5736.
11. A. M. Maurer-Jones, Y. S. Lin and C. L. Haynes, *ACS Nano*, **2010**, *4*, 3363–3373.
12. Y. Habibi, L. A. Lucia and O. J. Rojas, *Chem. Rev.*, **2010**, *110*, 3479–3500.

13. J. B. Zeng, Y. S. He, S. L. Li and Y. Z. Wang, *Biomacromolecules*, **2012**, *13*, 1−11.
14. I. S. Yeo, J. E. Oh, L. Jeong, T. S. Lee, S. J. Lee, W. H. Park and B. M. Min, *Biomacromolecules*, **2008**, *9*, 1106-1116.
15. X. Z. Xu, F. Liu. L. Jiang. J. Y. Zhu, D. Haagenson and D. P. Wiesenborn, *ACS Appl. Mater. Interfaces*, **2013**, *5*, 2999−3009.
16. H. Jin, A. Cao, E. Shi, J. Seitsonen, L. Zhang, R. H. A. Ras, L. A. Berglund, M. Ankerfors, A. Waltherf and O. Ikkala, *J. Mater. Chem. B*, **2013**, *1*, 835−840.
17. N. Lin and A. Dufresne, *Macromolecules*, **2013**, *46*, 5570−5583.
18. M. Martínez-Sanz, A. Lopez-Rubio and J. M. Lagaron, *Biomacromolecules*, **2012**, *13*, 3887−3899.
19. H. Lee, S. M. Dellatore, M. W. Miller and P. B. Messersmith, *Science*, **2007**, *318*, 426-430.
20. D. R. Dreyer, D. J. Miller, B. D. Freeman, D. R. Paul and C. W. Bielawski, *Chem. Sci.*, **2013**, *4*, 3796-3802.
21. Q. Liu, B. Huang and A. Huang, *J. Mater. Chem. A*, **2013**, *1*, 11970–11974.
22. X. C. Liu, G. C. Wang, R. P. Liang, L. Shi and J. D. Qiu., *J. Mater. Chem. A*, **2013**, *1*, 3945–3953.
23. N. F. D. Vecchia, R. Avolio, M. Alfè, M. E. Errico, A. Napolitano and M. d'Ischia, *Adv. Funct. Mater.*, **2013**, *23*, 1331–1340.
24. J. Liebscher, R. Mrówczyński, H. A. Scheidt, C. Filip, N. D. Hădade, R. Turcu, A. Bende and S. Beck, *Langmuir*, **2013**, *29*, 10539−10548.
25. M. H. Ryou, Y. M. Lee, J. K. Park and J. W. Choi, *Adv. Mater.*, **2011**, *23*, 3066–3070.
26. J. W. Cui, Y. Yan, K. G. Such, K. Liang, J. C. Ochs, A. Postma and F. Caruso, *Biomacromolecules*, **2012**, *13*, 2225−2228.
27. R. J. Li, K. Parvez, F. Hinkel, X. L. Feng and K. Müllen, *Angew. Chem. Int. Ed.*, **2013**, *52*, 5535 –5538.
28. V. K. Thakur, J. Yan, M. F. Lin, C. Y. Zhi, D. Golberg, Y. Bando, R. Sim and P. S. Lee, *Polym. Chem.*, **2012**, *3*, 962–969.
29. H. Y. Hu, B. Yu, Q. Ye, Y. S. Gu and F. Zhou, *Carbon*, **2010**, *48*, 2347–2353.
30. M. Lee, S. H. Ku, J. K. Ryu and C. B. Park, *J. Mater. Chem.*, **2010**, *20*, 8848–8853.
31. L. Guo, Q. Liu, G. Li, J. Shi, J. Liu, T. Wang and G. Jiang, *Nanoscale*, **2012**, *4*,

5864–5867.

32. S. M. Kang, S. J. Park, D. Kim, S. Y. Park, S. R. Ruoff and H. Lee, *Adv. Funct. Mater.*, **2011**, *21*, 108–112.
33. L. Q. Xu, W. J. Yang, K. G. Neoh, E. T. Kang and G. D. Fu, *Macromolecules*, **2010**, *43*, 8336–8339.
34. L. P. Yang, S. L. Phua, J. K. H. Teo. C. L. Toh, S. K. Lau, J. Ma and X. H. Lu, *ACS Appl. Mater. Interfaces*, **2011**, *3*, 3026–3032.
35. S. L. Phua, L. P. Yang, C. L. Toh, G. Q. Ding, S. K. Lau, D. Aravind and X. H. Lu, *ACS Appl. Mater. Interfaces*, **2013**, *5*, 1302−1309.
36. S. L. Phua, L. P. Yang, C. L. Toh, S. Huang, T. Zviad, S. K. Lau, Y. W. Mai and X. H. Lu, *ACS Appl. Mater. Interfaces*, **2012**, *4*, 4571−4578.
37. J. Wünsche, F. Cicoira, C. F. O. Graeff and C. Santato, *J. Mater. Chem. B*, **2013**, *1*, 3836–3842.
38. K. Y. Ju, Y. Lee, S. Lee, S. B. Park and J. K. Lee, *Biomacromolecules*, **2011**, *12*, 625–632.
39. K. Shanmuganathan, J. H. Cho, P. Iyer, S. Baranowitz and C. J. Ellison, *Macromolecules*, **2011**, *44*, 9499–9507.
40. M. d'Ischia, A. Napolitano, A. Pezzella, P. Meredith and T. Sarna, *Angew. Chem. Int. Ed.*, **2009**, *48*, 3914 – 3921.
41. J. P. Bothma, J. de Boor, U. Divakar, P. E. Schwenn, and P. Meredith, *Adv. Mater.*, **2008**, *20*,3539–3542.
42. J. Yan, L. P. Yang, M. F. Lin, J. Ma, X. H. Lu and P. S. Lee, *Small*, **2013**, *9*, 596–603.
43. K. L. Ai, Y. L. Liu, C. P. Ruan, L. H. Lu and G. Q. Lu *Adv. Mater.*, **2013**, *25*, 998–1003.
44. A. J. Uddin, J. Araki and Y. Gotoh, *Biomacromolecules*, **2011**, *12*, 617–624.
45. T. Terao, Y. Bando, M. Mitome, C. Y. Zhi, C. C. Tang and D. Golberg, *J. Phys. Chem. C*, **2009**, *113*, 13605–13609.
46. U. Siripatrawan and B. R. Harte, *Food Hydrocolloids*, **2010**, *24*, 770-775.
47. P. Sonkaew, A. Sane and P. Suppakul, *J. Agric. Food Chem.*, **2012**, *60*, 5388− 5399.
48. R. A. Zangmeister, T. A. Morris and M. J. Tarlov, *Langmuir*, **2013**, *29*, 8619−8628.
49. H. Chao and R. A. Riggleman, *Polymer*, **2013**, *54*, 5222-5229.

50. T. N. Zhou, F. Chen, C. Y. Tang, H. W. Bai, Q. Zhang, H. Deng and Q. Fu, *Compos. Sci. Technol.*, **2011**, *71*, 1266-1270.
51. H. J. Salavagione, G. Martínez and M. A. Gómez, *J. Mater. Chem.*, **2009**, *19*, 5027–5032.
52. M. S. Peresin, Y. Habibi, A. H. Vesterinen, O. J. Rojas, J. J. Pawlak and J. V. Seppälä, *Biomacromolecules*, **2010**,*11*,2471–2477.
53. S. Bandi, and D. A. Schiraldi, *Macromolecules*, **2006**, *39*, 6537-6545.
54. L. Chen, K. Zheng, X. Y. Tian, K. Hu, R. X. Wang, C. Liu, Y. Li and P. Cui, *Macromolecules*, **2010**, *43*, 1076–1082.
55. S. Bhattacharyya, J. P. Salvetat and M. L. Saboungi, *Appl. Phys. Lett.*, **2006**, *88*, 233119-1–3.
56. J. Z. Xu, T. Chen, C. L. Yang, Z. M. Li, Y. M. Mao, B. Q. Zeng and S. H. Benjamin, *Macromolecules*, **2010**, *43*, 5000–5008.
57. S. Pandey, S. K. Pandey, V. Parashar, G. K. Mehrotra and A. C. Pandey, *J. Mater. Chem.*, **2011**, *21*, 17154–17159.
58. P. Zheng and X. K. Ling, *Polym. Degrad. Stab.*, **2007**, *92*, 1061-1071.
59. A. Li, Y. Z. Pan, X. W. Shen, H. B. Lu and Y. L. Yang, *J. Mater. Chem.*, **2008**, *18*, 4928–4941.
60. C. K. Chozhan, M. Alagar and P. Gnanasunda, *Acta Mater.*, **2009**, *57*, 782–794.
61. H. W. P. Carvalho, C. V. Santilli, V. Briois and S. H. ulcinelli, *RSC Adv.*, **2013**, *3*, 22830 – 22833.
62. F. Tian, E. A. Decker and J. M. Goddard, *J. Agric. Food Chem.*, **2011**, *59*, 7832–7840.
63. E. Portes, C. Gardrat, A. Castellan and V. Coma, *Carbohyd. Polym.*, **2009**, *76*, 578-584.
64. Y. Byun, Y. T. Kim and S. Whiteside, *J. Food Eng.*, **2010**, *100*, 239–244.
65. A. Hambardzumyan, L. Foulon, B. Chabbert and V. Aguié-Béghin, *Biomacromolecules*, **2012**, *13*, 4081− 4088.
66. F. Aloui, A. Ahajji, Y. Irmouli, B. George, B. Charrier and A. Merlin, *Appl. Surf. Sci.*, **2007**, *253*, 3737-3745.
67. Y. Tu, L. Zhou, Y. Z. Jin, C. Gao, Z. Z. Ye, Y. F. Yang and Q. L. Wang, *J. Mater. Chem.*, **2010**, *20*, 1594–1599.

68. S. H. Li, M. S. Toprak, Y. S. Jo, J. Dobson, D. K. Kim and M. Muhammed, *Adv. Mater.*, **2007**, *19*, 4347–4352.
69. X. Wang, S. Zhou and L. Wu, *J. Mater. Chem. C*, **2013**, *1*, 7547–7553.
70. G. Johnsy, K. K. R. Datta, V. A. Sajeevkumar, S. N. Sabapathy, A. S. Bawa, and M. Eswaramoorthy, *ACS Appl. Mater. Interfaces*, **2009**, *1*, 2796-2803.
71. Z. H. Tang, Y. D. Lei, B. C. Guo, L.Q. Zhang and D. M. Jia, *Polymer*, **2012**, *53*, 673-680.
72. M. Cadek, J. N. Coleman, K. P. Ryan, V. Nicolosi, G. Bister, A. Fonseca, J. B. Nagy, K. Szostak, F. Béguin, W. J. Blau, *Nano Lett.*, **2004**, *4*, 353-356.
73. F, K. Yang, W. Zhang, Y. Han, S. Yoffe, Y. Cho and B. X. Zhao, *Langmuir*, **2012**, *28*, 9562−9572.

Table 1. Thermal properties of PDAP/PVA composites extracted from DSC measurements.

PDAP contents	*ΔHm* (J/g)	*Xc*(%), Heatig Scan	*ΔHm2* (J/g)	*Xc*(%), Cooling Scan	*Tg* (℃)	*Tm* (℃)	*Tc* (℃)
0	34.7	25.0	20.7	14.9	43.3	231.3	165.9
PDAP-1-5wt%	48.7	35.1	35.0	25.3	45.2	232.5	180.4
PDAP-1-10wt%	59.5	42.9	39.9	28.8	45.8	235.3	186.7
PDAP-1-15wt%	63.0	45.4	51.0	36.8	47.4	236.2	189.8
PDAP-2-5wt%	50.2	36.2	30.1	23.7	44.4	232.0	175.7
PDAP-2-10wt%	57.9	41.8	38.2	27.6	45.4	233.4	186.1
PDAP-2-15wt%	58.6	42.3	45.5	32.8	48.6	234.6	190.3

Table 2. Physical properties of pure PVA and PDAP/PVA composites

PDAP contents	Tensile strength (MPa)	Tensile modulus (GPa)	Elongation at break (%)	Ts (℃)	T_{max} (℃)
0	37±4	1.12±0.03	180.7±11.3	248.3	263.3
PDAP-1-5wt%	44±5	1.32±0.09	109.2±7.8	258.8	277.1
PDAP-1-10wt%	55±7	1.44±0.06	98.5±8.1	269.2	292.3
PDAP-1-15wt%	61±5	1.77±0.02	73.3±6.5	277.5	309.3
PDAP-2-5wt%	44±4	1.34±0.10	106.6±5.3	258.0	285.5
PDAP-2-10wt%	48±6	1.35±0.06	92.7±6.6	273.3	298.1
PDAP-2-15wt%	59±4	1.72±0.01	84.6±5.6	278.1	305.9

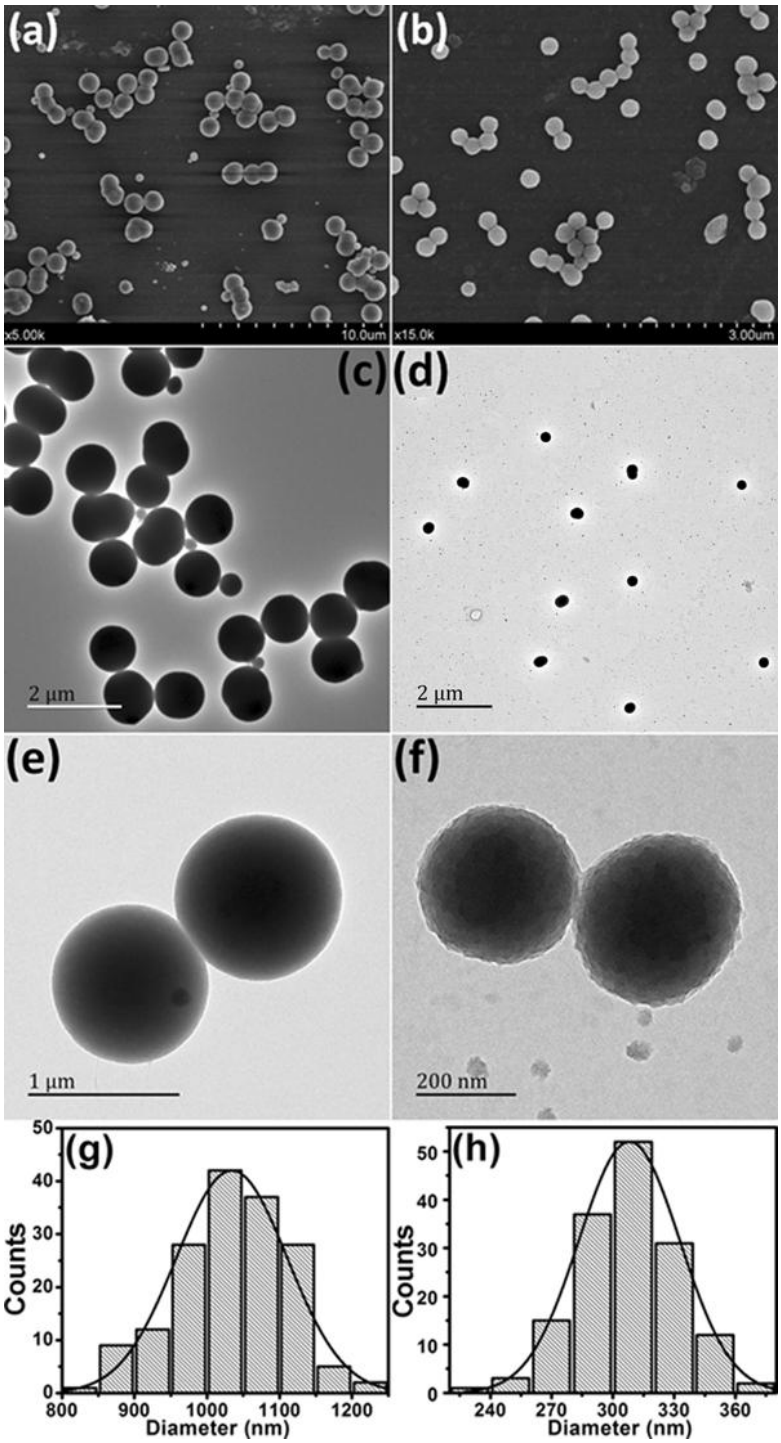

Figure 1. (a) SEM image of PDAP-1. (b) SEM image of PDAP-2. (c, e) TEM images of PDAP-1. (d,f) TEM images of PDAP-2. (g) Size distribution derived from SEM and TEM images of PDAP-1. (h) Size distribution derived from SEM and TEM images of PDAP-2.

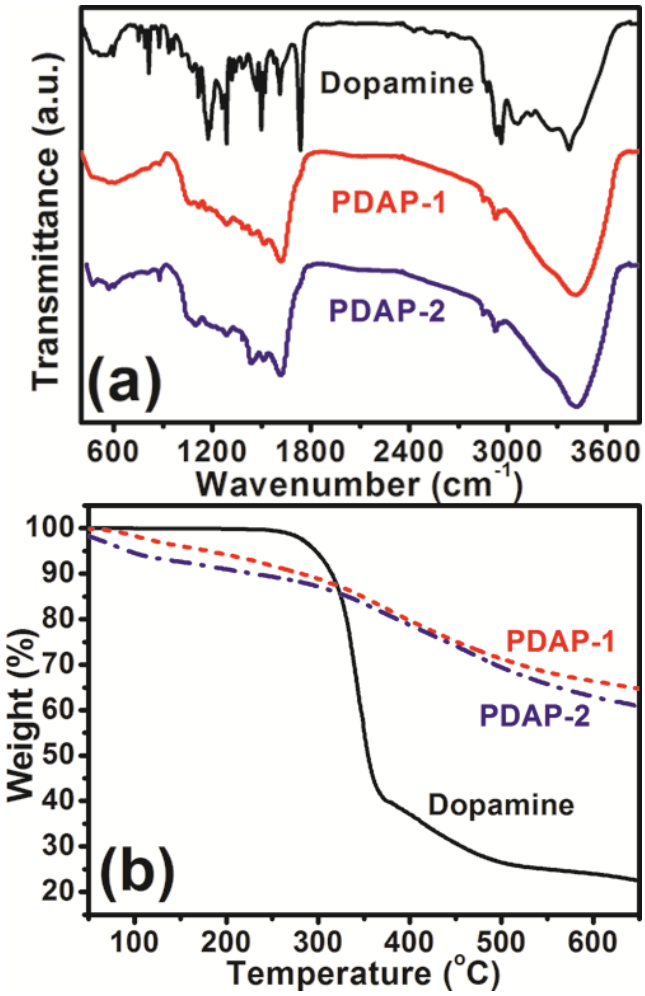

Figure 2. FT-IR spectra (a) and TGA curves (b) of PDAP-1 and PDAP-2.

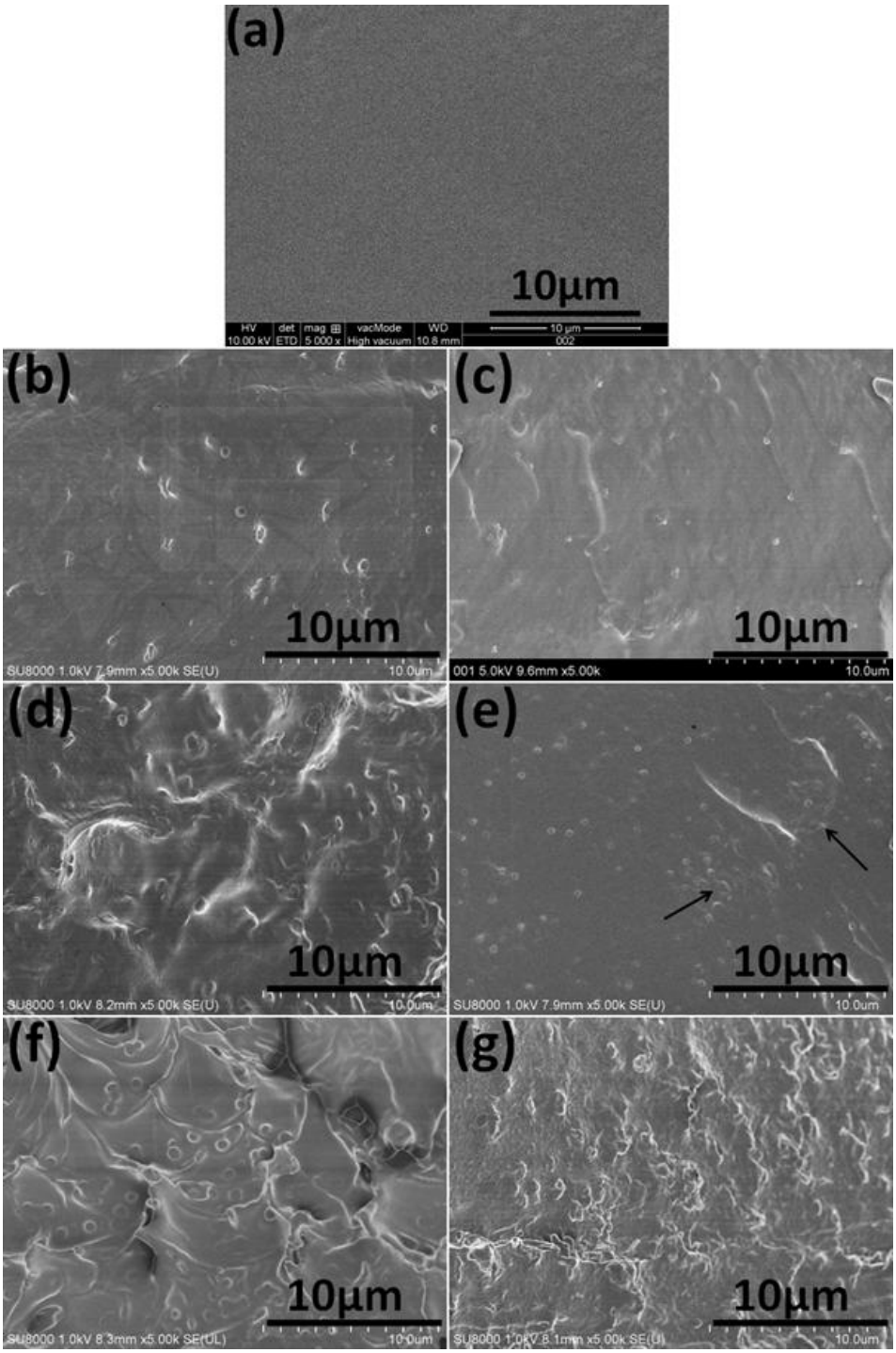

Figure 3. SEM images of the fracture surfaces of (a) PVA, composites with (b) 5 wt%, (d) 10 wt%, (f) 15 wt% PDAP-1, and composites with (c) 5 wt%, (e) 10 wt%, and (g) 15 wt% PDAP-2.

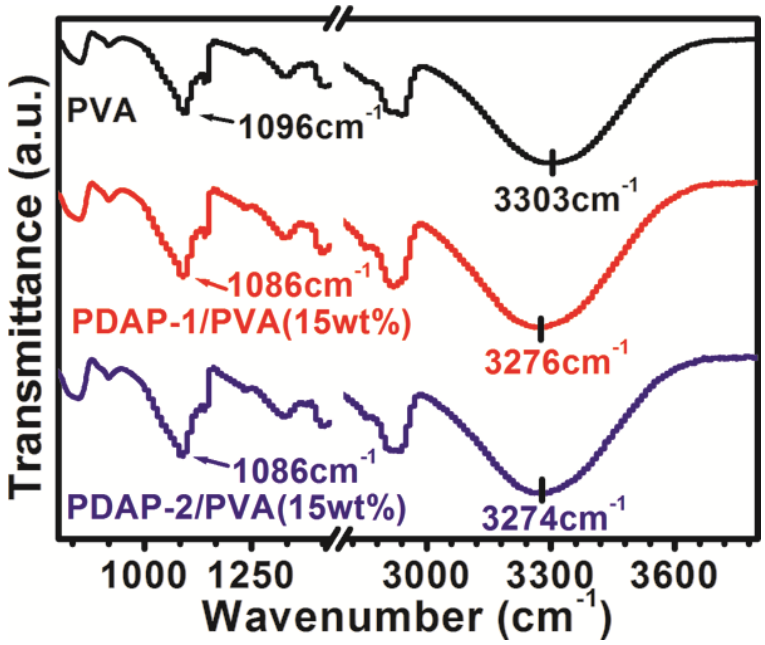

Figure 4. FT-IR spectra of PVA, PDAP-1/PVA and PDAP-2/PVA composites with 10 wt% filler loading.

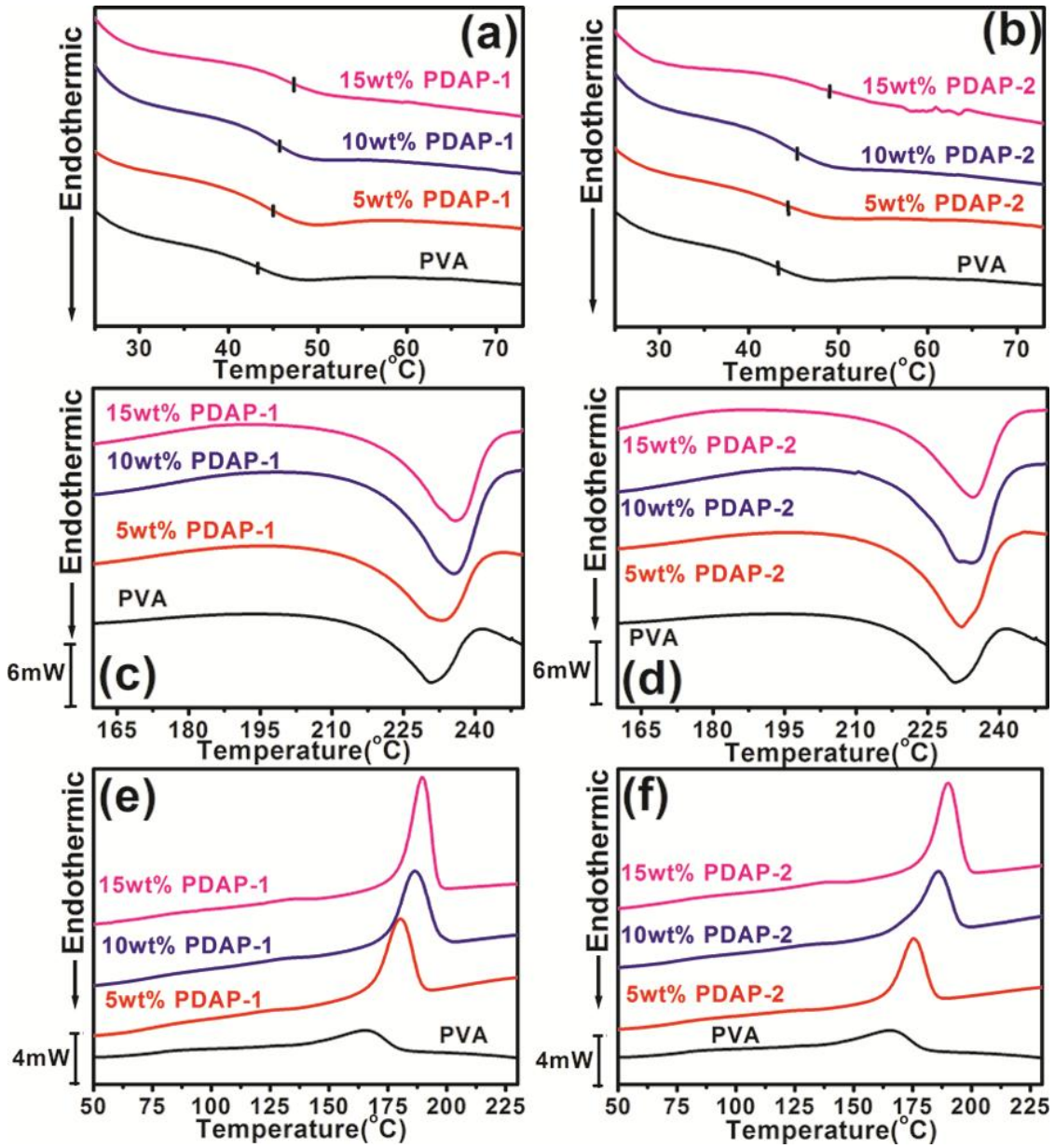

Figure 5. (a, c) DSC curves of heating scans of PDAP-1/PVA composites. (b, d) DSC curves of heating scans of PDAP-2/PVA composites. (e) DSC curves of cooling scans of PDAP-1/PVA composites. (f) DSC curves of cooling scans of PDAP-2/PVA composites.

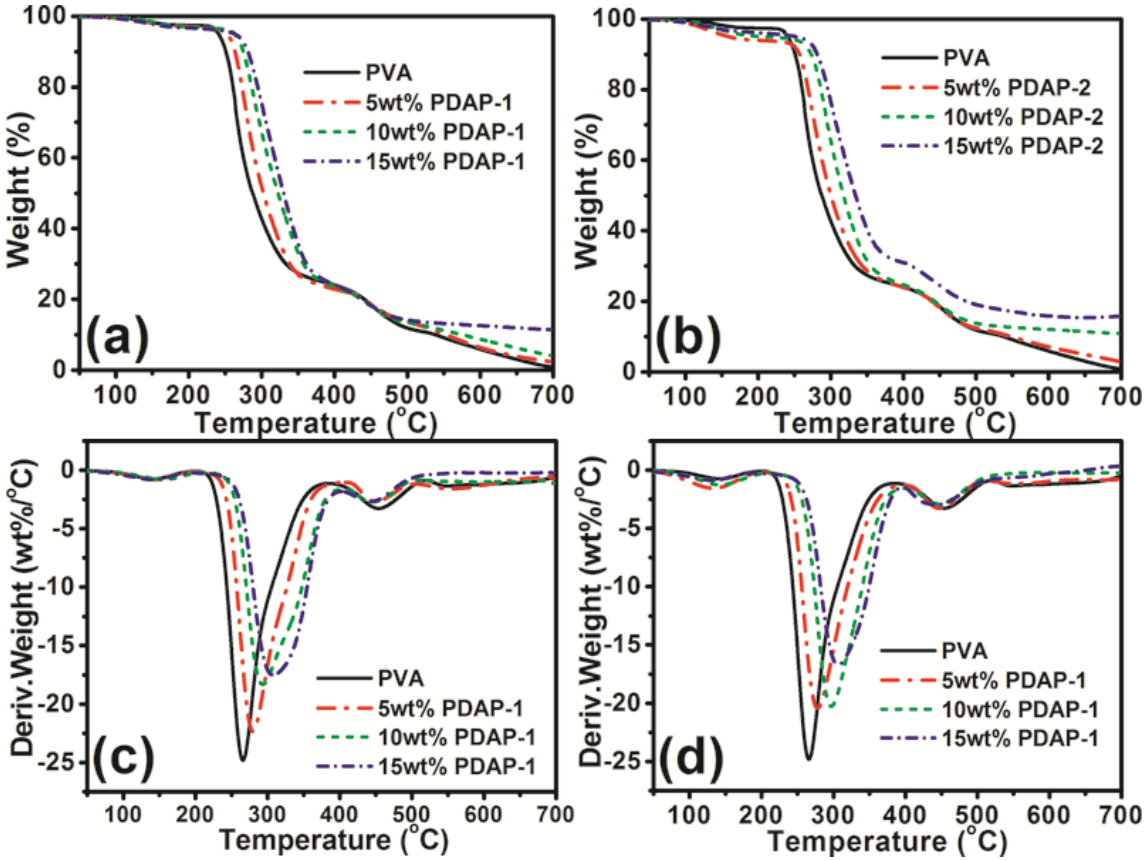

Figure 6. (a) Thermogravimetric analysis and (c) derivative thermo- gravimetric analysis plots of PVA and PDAP-1/PVA composites, (b) Thermogravimetric analysis and (d) derivative thermogravimetric analysis plots of PVA and PDAP-2/PVA composites.

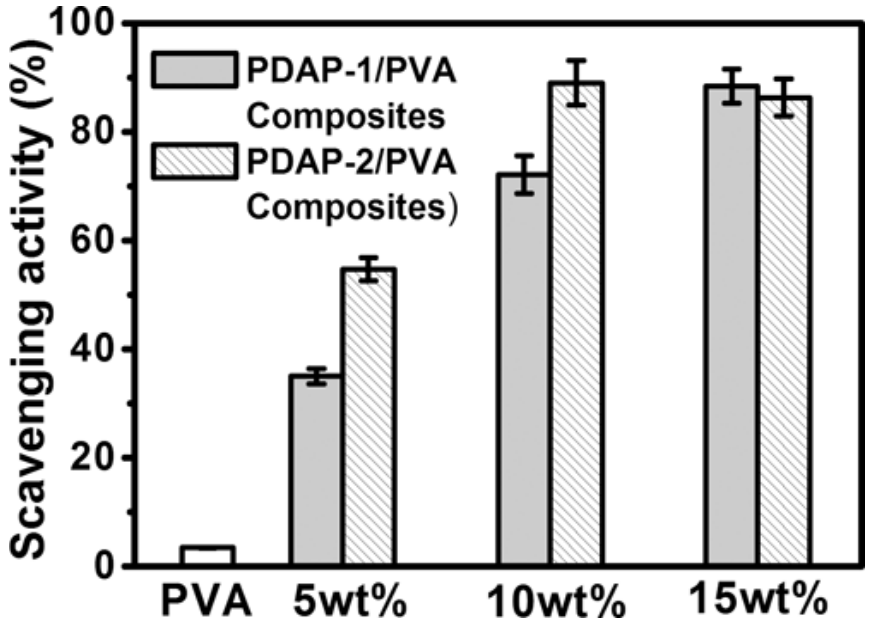

Figure 7. DPPH radical scavenging activity of PVA and PDAP/PVA composites.

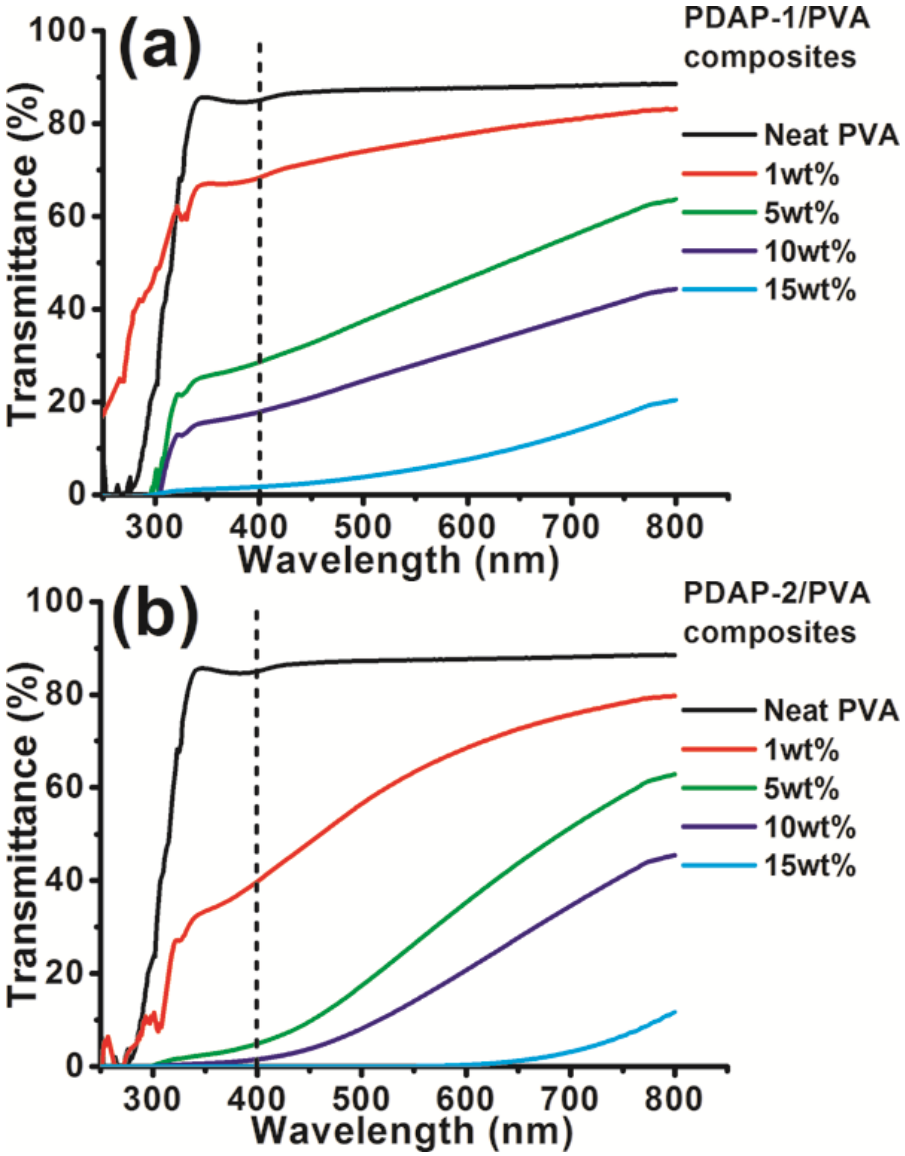

Figure 8. UV-Vis transmittance spectra of (a) PDAP-1/PVA and (b) PDAP-2/PVA composites.

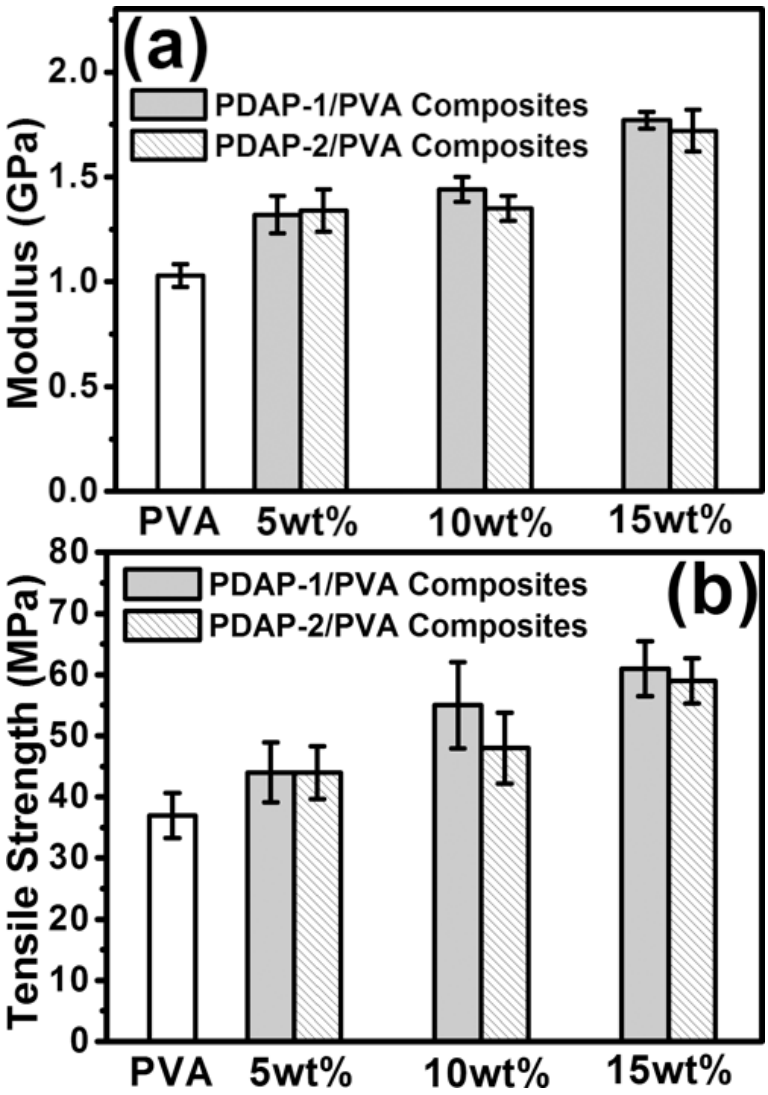

Figure 9. Comparison of (a) modulus and (b) tensile strength of different composites.

Graphical Abstract

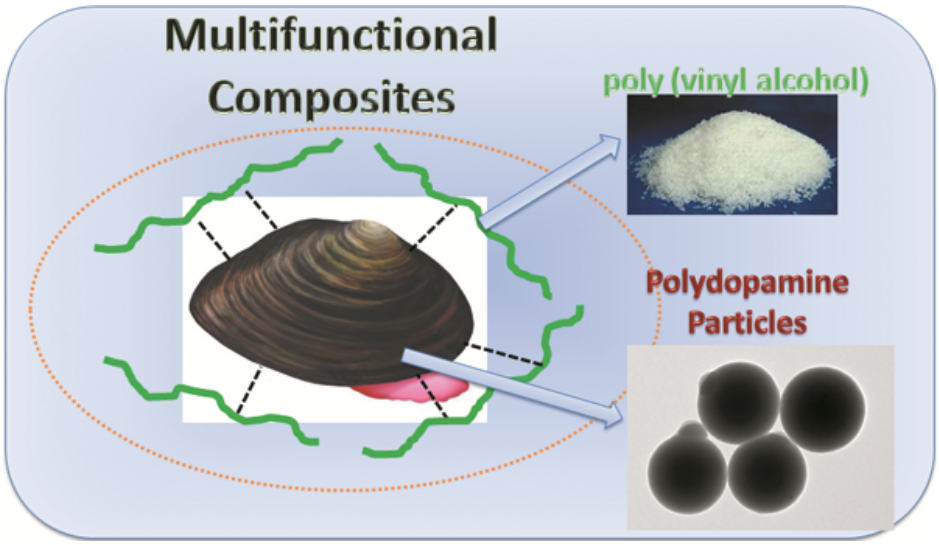

Polydopamine particles were used as fillers for constructing multifunctional composites for the first time